

Investigation of Current Re-Distribution in
Super-Stabilized Superconducting Winding When
Switching to the Normal Resistive State *

A. Devred
SSC Central Design Group
c/o UCLBL, MS 90-4040
One Cyclotron Road
Berkeley, CA 94720
U.S.A.

September 1988

Abstract

We have investigated the electro-magnetic behavior of a layer of super-stabilized superconductive composite conductors when switching instantaneously and uniformly to the normal resistive state. The Laplace transform was used to solve the current diffusion equation in the super-stabilizing material. The value of power dissipated per unit volume, averaged over the layer thickness, was then computed using the "pseudo"-convolution theorem in the complex plane. Last, we present a simple interpretation of the phenomenon with the help of two time constants.

* This work is part of "Longitudinal Propagation of the Normal Zone through Indirectly Cooled Superconducting Solenoids," a Ph.D. thesis completed at the Commissariat à l'Énergie Atomique, CEN/Saclay, D.Ph.P.E./STIPE/STCM, 91 191 Gif-sur-Yvette Cédex (France).

Introduction

When a superconductive composite material switches to the normal resistive state, the larger part of the current diffuses from the filaments into the copper. Early in the period following the transition, dissipated power is significantly higher than the residual power remaining after the diffusion process has been completed. This excess power may affect the stability of the composite material.¹⁻⁴ In the case of super-stabilized conductors, such as the "ALEPH" conductor,⁵ in which the composite material is enclosed in large volume of pure aluminum, the magnetic diffusion characteristic time becomes large in comparison with the normal zone propagation characteristic time. The cryogenic stability problem is thus compounded by propagation velocity considerations.

In an earlier paper,⁶ we have shown how the propagation velocity along a layer of such conductors (see Fig. 1) can be related to the Laplace transform of the value of power dissipated per unit volume, averaged over the layer thickness. We have also shown that an asymptotic limit mode can be reached, in which the power profile to be considered is that derived by assuming that the superconductor layer switches uniformly at time $t = 0$. The purpose of this investigation was to determine this power profile.

Geometrical Model and Computational Assumptions

The model and assumptions given in our earlier paper⁶ were used again in this case. Subscripts 1 and 2 refer to the composite and super-stabilizing materials respectively.

It was assumed that the electro-magnetic behavior of the conductor layer in Fig. 1 was similar to that of the set of infinite plates of Fig. 2. Therefore, electro-magnetic values are dependent on variables y and t only, and the Maxwell-Ampere equation for quasi-steady states shows the only components of interest to be the magnetic flux density component along Ox and the current density component along Oz . These two components are designated respectively as $B_i(y, t)$ and $J_i(y, t)$ where $i = 1$ or 2 .

At any time $t \geq 0$, the composite material is regarded as a homogeneous medium with equivalent longitudinal resistivity, ρ_1 , in which current density is uniform. This last assumption is equivalent to considering that diffusion through the copper in the composite material following a transition is instantaneous on the time scale of diffusion through the

super-stabilizer. The range of validity of that assumption will be defined later. As regards the super-stabilizer, it is characterized by its magnetic diffusivity:

$$D_m = \rho_2 / \mu_o \quad (\text{m}^2\text{s}^{-1})$$

It was also assumed that a constant current I flows through the winding during the whole process. We call J_o the average current density across plate thickness $2L$, and write $B_o = -\mu_o J_o L$, where J_o and B_o are constants. The flat plate model being extrapolated from a large solenoid, we define half-space $y > L$ outside the solenoid, where flux density is nil, and half-space $y < -L$ inside the solenoid, where flux density is $(-2B_o)$. We then establish symmetry with respect to y (in this case, odd as regards B and even as regards J) by superimposing a uniform, constant flux density equal to B_o . The investigation was performed in the $y \geq 0$ half-space.

The numerical data used are those tabulated opposite; they relate to a model of the "ALEPH" solenoid.^{5,6}

Throughout the following, the Laplace transform of a function $f(t)$ is written $f^*(p)$.

Determination of Flux Density

1. Equations and Boundary Conditions

Inside the composite material, where current density is assumed to be uniform, $B_1(y, t)$ varies linearly with respect to y . The odd symmetry conditions, and the conservation of the flux density normal component at $y = L_1$ yield

$$B_1(y, t) = B_2(y, t) \frac{y}{L_1} \quad \forall y, 0 \leq y \leq L_1; \forall t, t \geq 0$$

Inside the super-stabilizer, $B_2(y, t)$ is a solution of the magnetic diffusion equation (E)

$$\frac{\partial^2 B_2(y, t)}{\partial y^2} = \frac{1}{D_m} \frac{\partial B_2(y, t)}{\partial t} \quad \forall y, L_1 \leq y \leq L; \forall t, t \geq 0$$

with the three boundary conditions 1) at $t = 0$, when current is still confined to the composite: $B_2(y, t = 0) = B_o$; 2) at $y = L$: $B_2(y = L, t) = B_o$; 3) at $y = L_1$, where conservation of the electric field tangential components affects current density according to Ohm's law, and flux density according to the Maxwell-Ampere equation, giving

$$B_2(y = L_1, t) = \frac{\rho_2 L_1}{\rho_1} \frac{\partial B_2(y = L_1, t)}{\partial y}$$

2. Computation of the Laplace Transform

Multiplying equation (E) and conditions 2) and 3) by $Y(t)$, the Heaviside step function, we derive the Laplace transform with respect to t . We then solve (E) as a differential equation of the second order with respect to y . The calculations give

$$B_1^*(y, p) = B_0 \sqrt{\frac{\tau_1}{p}} \frac{ch\sqrt{\tau_2 p}}{sh\sqrt{\tau_2 p} + \sqrt{\tau_1 p} ch\sqrt{\tau_2 p}} \frac{y}{L_1}$$

$$B_2^*(y, p) = \frac{B_0}{p} \left\{ 1 - \frac{sh\left(\frac{L-y}{\sqrt{D_m}} \sqrt{p}\right)}{sh\sqrt{\tau_2 p} + \sqrt{\tau_1 p} ch\sqrt{\tau_2 p}} \right\}$$

where

$$\tau_1 = \left(\frac{\rho_2}{\rho_1}\right)^2 \frac{L_1^2}{D_m} \quad \text{and} \quad \tau_2 = \frac{L_2^2}{D_m}$$

(τ_1 and τ_2 have the dimension of time).

Note: in the case of interest, $\rho_2 < \rho_1$ and $L_1 \ll L_2$, hence $\tau_1 \ll \tau_2$.

3. Computing the Original

The Laplace transform inversion formula is written

$$B_i(y, t) = \frac{1}{2_j \pi} \int_{c-j\infty}^{c+j\infty} dp \exp(pt) B_i^*(y, p) \quad i = 1 \text{ or } 2$$

integrating along a straight line $x = c$, such that $c > \sigma(B_i^*)$ where $\sigma(B_i^*)$ is the B_i^* summability abscissa, i.e., a point such that all the singularities of B_i^* are located left of that line.

From the above expressions, B_i^* shows a pole at zero, and an infinitive number of poles $(p_n)_{n \in \mathbb{N}}$ on the negative real half-axis, given by $p_n = -\alpha_n^2/\tau_2$ where α_n is the solution of equation $tg \alpha_n = -m\alpha_n$ located in the interval $[(n + 1/2)\pi, (n + 3/2)\pi]$ with $m = (\rho_2 L_1 / \rho_1 L_2)$. $\sigma(B_i^*)$ is therefore nil, and any strictly positive real value is adequate for c .

The integral is computed by considering the set of contours $(C_n(R_n))$ represented by Fig. 3.⁷ Each contour consists of a circular arc with center 0 and radius R_n (designated as $\Gamma_n(R_n)$), two straight segments parallel to the real axis (designated as $D_n(R_n)$) and the segment $[-R_n, +R_n]$ of line $x = c$.

Note: Although it may look so, B_i^* is not multiform, and it is not necessary to make a cut-off on the contours. We therefore have

$$B_i(y, t) = \lim_{n \rightarrow +\infty} \left\{ \frac{1}{2j\pi} \left(\int_{C_n} - \int_{\Gamma_n} - \int_{D_n} \right) dp \exp(pt) B_i^*(y, p) \right\}$$

The integral over C_n is computed by the method of residues; and it can be verified that integrals over Γ_n and D_n tend toward zero when n tend toward infinity. We thus have:

$$B_i(y, t) = \text{Res}[\exp(pt) B_i^*(y, p), p = 0] + \sum_{n=0}^{+\infty} \text{Res}[\exp(pt) B_i^*(y, p), p = p_n]$$

Residue computation yields

$$B_1(y, t) = B_o \left\{ \frac{m}{1+m} + 2 \sum_{n=0}^{+\infty} \frac{m \exp(-\alpha_n^2 t / \tau_2)}{1+m+(m\alpha_n)^2} \right\} \frac{y}{L_1}$$

and

$$B_2(y, t) = B_o \left\{ 1 - \frac{\frac{L-y}{L_1}}{1+m} + 2 \sum_{n=0}^{+\infty} \frac{\sin\left(\frac{L-y}{L_1} \alpha_n\right)}{\sin \alpha_n} \frac{m \exp(-\alpha_n^2 t / \tau_2)}{1+m+(m\alpha_n)^2} \right\}$$

To arrive at the right expressions for flux density, it is now sufficient to subtract B_o .

Figure 4 shows $B = f(y)$ curves for miscellaneous values of t .

Determination of Current Density

The Maxwell-Ampere equation for quasi-steady states is written:

$$J_i(y, t) = -\frac{1}{\mu_o} \frac{\partial B_i(y, t)}{\partial y} \quad i = 1 \text{ or } 2$$

Derivating the above expansions on a term-by-term basis, we have

$$J_1(t) = J_o \frac{L}{L_1} \left\{ \frac{m}{1+m} + 2 \sum_{n=0}^{+\infty} \frac{m \exp(-\alpha_n^2 t / \tau_2)}{1+m+(m\alpha_n)^2} \right\}$$

and

$$J_2(y, t) = J_o \frac{\rho_1 L}{\rho_2 L_1} \left\{ \frac{m}{1+m} + 2 \sum_{n=0}^{+\infty} \frac{\cos\left(\frac{L-y}{L_1} \alpha_n\right)}{\cos \alpha_n} \frac{m \exp(-\alpha_n^2 t / \tau_2)}{1+m+(m\alpha_n)^2} \right\}$$

$J = f(y)$ curves for different values of t are shown in Fig. 5.

Also, $J_i^*(y, p)$ can be directly related to $\frac{\partial B_i^*(y, p)}{\partial y}$ by multiplying the Maxwell-Ampere equation by $Y(t)$, and deriving the Laplace transform with respect to t . We have

$$J_1^*(p) = J_0 \frac{L}{L_1} \sqrt{\frac{\tau_1}{p}} \frac{ch\sqrt{\tau_2 p}}{sh\sqrt{\tau_2 p} + \sqrt{\tau_1 p} ch\sqrt{\tau_2 p}}$$

and

$$J_2^*(y, p) = J_0 \frac{\rho_1 L}{\rho_2 L_1} \sqrt{\frac{\tau_1}{p}} \frac{ch\left(\frac{L-y}{\sqrt{D_m}} \sqrt{p}\right)}{sh\sqrt{\tau_2 p} + \sqrt{\tau_1 p} ch\sqrt{\tau_2 p}}$$

Determination of the Average Power Density

1. General Expression

Based on symmetry considerations, the power dissipated per unit volume, averaged across plate thickness, is given by:

$$P_J(t) = \frac{1}{L} \left\{ \rho_1 J_1^2(t) L_1 + \int_{L_1}^L dy \rho_2 J_2^2(y, t) \right\}$$

To compute $P_J^*(p)$, a first method consists on replacing $J_1(t)$ and $J_2(y, t)$ by the expansions derived above, and deriving the Laplace transform with respect to t . We thus obtain a serie's expansion of $P_J^*(p)$. The second method, which we develop here, consists on using the Laplace transform directly, and leads to a simple analytical expression. Of course, we have verified that these two computations gave coherent results.

2. Computing the Laplace Transform

P_J^* can be expressed as a function of $J_1^*(p)$ and $J_2^*(y, p)$ by using the "pseudo"-convolution theorem in the complex plane. This theorem relates the Laplace transform of a function to that of its square.⁷ We have

$$P_J^*(p) = \frac{1}{L} \left\{ \rho_1 L_1 \left(\frac{1}{2_j \pi} \int_{c-j\infty}^{c+j\infty} du J_1^*(u) J_1^*(p-u) \right) + \rho_2 \int_{L_1}^L dy \left(\frac{1}{2_j \pi} \int_{c-j\infty}^{c+j\infty} du J_2^*(y, u) J_2^*(y, p-u) \right) \right\}$$

integrating along a straight line $x = c$, such that $\sigma(J_1^*) < c < \text{Res}(p) - \sigma(J_2^*)$. Since the poles of J_i^* are the same as those of B_i^* , $\sigma(J_i^*) = 0$, and in the following we will take $c = \text{Res}(1/3 p)$.

Replacing $J_1^*(p)$ and $J_2^*(p)$ by the expressions found earlier inverting both integrations in the right side, and computing the integral with respect to y , P_J^* can be written in the form

$$P_J^*(p) = \frac{1}{2_j \pi} \left(\int_{\text{Res}(\frac{1}{3}p) - j\infty}^{\text{Res}(\frac{1}{3}p) + j\infty} + \int_{\text{Res}(\frac{1}{3}p) - j\infty}^{\text{Res}(\frac{1}{3}p) + j\infty} \right) du f(p, u)$$

where

$$f(p, u) = P_{J_0} \frac{g(u)}{u - p/2}$$

with

$$P_{J_0} = \rho_1 \frac{L}{L_1} J_0^2$$

(P_{J_0} is the average density of dissipated power at time $t = 0$.)

and

$$g(u) = -\frac{1}{2} \sqrt{\frac{\tau_1}{u}} \frac{ch\sqrt{\tau_2 u}}{sh\sqrt{\tau_2 u} + \sqrt{\tau_1 u} ch\sqrt{\tau_2 u}}$$

Note: The poles of $g(u)$ are zero, and the expansion $(p_n)_{n \in \mathbb{N}}$, $g(u)$ is therefore holomorphic in the $\text{Res}(u) > 0$ half plane.

The poles of $f(p, u)$ with respect to u are $p/2$ and those of $g(u)$.

In the following, we designate by $I(p)$ (resp. $K(p)$) the integral along line $x = \text{Res}(1/3 p)$ (resp. $x = \text{Res}(2/3 p)$).

• Computation of $K(p)$:

Let us consider contour $C_K(R)$ of Fig. 6a, and call $\Gamma_K(R)$ the fraction of this contour consisting of the circular arc with radius R . We thus have:

$$K(p) = - \lim_{R \rightarrow \infty} \left\{ \frac{1}{2_j \pi} \int_{C_K(R)} du f(p, u) - \frac{1}{2_j \pi} \int_{\Gamma_K(R)} du f(p, u) \right\}$$

Since $f(p, u)$ is holomorphic within the domain delineated by $C_K(R)$, the integral over $C_K(R)$ is nil.

Further considering that $th\sqrt{u} \simeq 1$ for $\text{Res}(u) \geq 0$ and $|u| \rightarrow +\infty$, we have $f(p, u) \simeq -P_{J_0}/(2u^2)$ for $u \in \Gamma_K(R)$ and $R \rightarrow +\infty$. Therefore $uf(p, u)$ tends uniformly toward zero over $\Gamma_K(R)$ when $R \rightarrow +\infty$ which is sufficient condition⁸ for the integral over $\Gamma_K(R)$ also to tend toward zero.

We therefore have: $K(p) = 0$.

• Computation of $I(p)$

Let us now consider $C_I(Y)$ in Fig. 6b, and call $D_I(Y)$ the fraction of that contour consisting of the two straight segments parallel to the real axis. We thus have:

$$I(p) = - \lim_{Y \rightarrow +\infty} \left\{ \frac{1}{2_j \pi} \int_{C_I(Y)} du f(p, u) - \frac{1}{2_j \pi} \int_{D_I(Y)} du f(p, u) \right\} + K(p)$$

The integral over $D_I(Y)$ tends toward zero when $Y \rightarrow +\infty$, for the same reasons as the integral over $\Gamma_K(R)$.

Further, $g(u)$ being holomorphic in the domain delineated by $C_I(Y)$, the integral over $C_I(Y)$ is computed by Cauchy's formula

$$\frac{1}{2_j \pi} \int_{C_I(Y)} du f(p, u) = \frac{1}{2_j \pi} \int_{C_I(Y)} du P_{J_0} \frac{g(u)}{u - p/2} = P_{J_0} g(p/2)$$

We thus have:

$$I(p) = - P_{J_0} g(p/2)$$

and finally, for $P_J^*(p)$:

$$P_J^*(p) = P_{J_0} \sqrt{\frac{\tau_1}{2}} \frac{1}{\sqrt{p}} \frac{ch \sqrt{\frac{\tau_1}{2p}}}{sh \sqrt{\frac{\tau_1}{2p}} + \sqrt{\frac{\tau_1}{2p}} ch \sqrt{\frac{\tau_1}{2p}}}$$

3. Computation of Original

The expression for P_J^* being of the same form as those for $B_1^*(y, p)$ and $J_1^*(p)$, it follows that:

$$P_J(t) = P_{J_{ss}} + 2 P_{J_0} \sum_{n=0}^{+\infty} \frac{m \exp(-2\alpha_n^2 t / \tau_2)}{1 + m + (m\alpha_n)^2}$$

in which we have written $P_{J_{ss}} = \frac{1}{1+m} P_{J_0}$ ($P_{J_{ss}}$ is the average power density at the end of the diffusion process).

Figure 7 shows the curve $P_J = f(t)$.

4. Approximate Expression

An approximate expression for $P_J(t)$ can be derived by connecting a truncated expansion for t , close to zero, and an asymptotic expansion for t close to infinity.

The truncated expansion is derived from the original of an approximate expression for $P_J^*(p)$, where $\text{Res}(p)$ is large. Assuming that $th(\sqrt{p})$ is equal to 1, we have

$$P_J^*(p) \simeq P_{J_0} \frac{1}{\sqrt{p}} \frac{1}{\sqrt{p} + \frac{1}{\sqrt{\tau_1}}}$$

where $\text{Res}(p)$ is large.

A table of transforms⁷ thus gives:

$$P_J(t) \simeq P_{J_0} \exp\left(\frac{2}{\tau_1} t\right) \text{erfc} \sqrt{\frac{2}{\tau_1} t}$$

where t is small and where

$$\text{erfc}(x) = \frac{2}{\sqrt{\pi}} \int_x^{+\infty} ds \exp(-s^2)$$

Note: Truncated expansions for $B_i(y, t)$ and $J_i(y, t)$ can be derived in the same way for t close to zero; in the super-stabilizer, however, a distinction should be made based on closeness of y to L_1 or L .

The asymptotic expansion is derived by retaining only the first term of the above expansion.

$$P_J(t) \simeq P_{J_{ss}} + 2 P_{J_0} \frac{m \exp(-2\alpha_0^2 t / \tau_2)}{1 + m + (m\alpha_0)^2} \quad \text{where } t \gg 2\alpha_1^2 / \tau_2$$

A plot of the above two expansions shows that they are connected, and sufficient to build the profile of Fig. 7.

At this point, we can see that there are two phases in the decay of the average density: a fast decay phase, with time constant τ_1 , and a slow decay phase with time constant τ_2 . The first phase may be interpreted as the forcing of the current out of the composite and into the super-stabilizer; as was pointed out earlier, $J_1^*(p)$ and $P_J^*(p)$ formally have the same expression. In particular, $J_1(t)$ has practically reached its limit after a few tens of τ_1 . This is because excess current has been driven from the composite during that period. As for the second phase, it is simply a diffusion phase in the super-stabilizer. (See the definition of τ_2).

This interpretation also permits determining the validity range of our uniform current density model for the composite. In fact, the model only appears to make sense if $\tau_1 \ll \tau_2$ which can be written:

$$m^2 \ll 1$$

The above relationship defines a super-stabilization criterion.

Conclusion

Using the Laplace transform, we have been able to solve the problem completely without having to use a computer. Further, the results obtained are of a simple form, which permits physical interpretations. Our method thus compares very favorably with others, especially with the variable separation method.

Acknowledgment

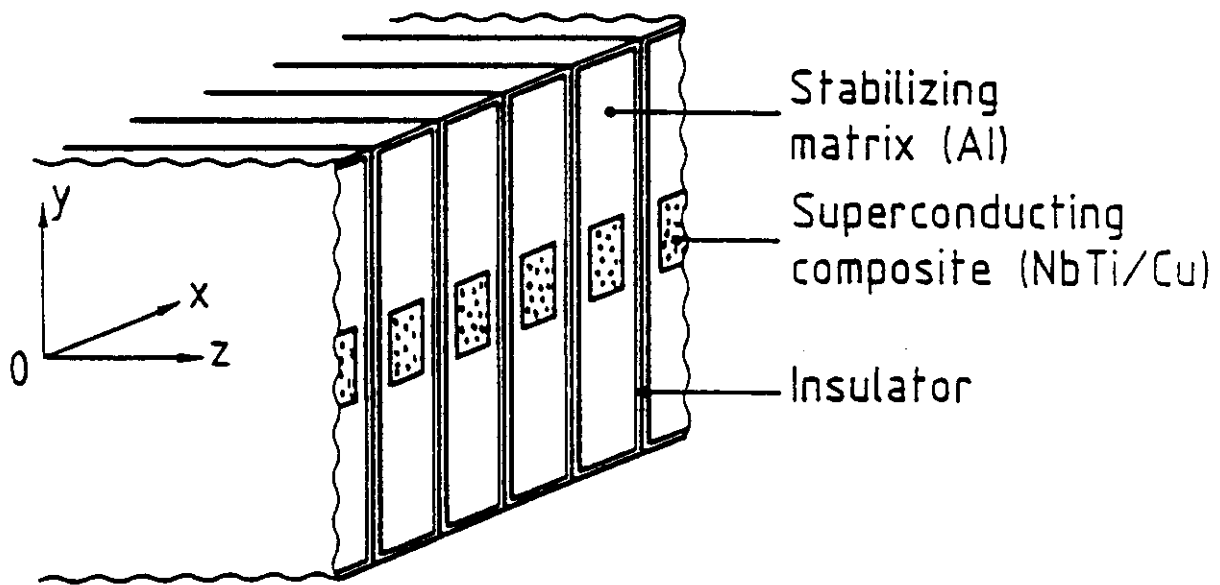
The SSC Central Design Group is operated by the Universities Research Association, Inc., under contract with the U.S. Department of Energy.

References

1. M. A. Hilal and R. W. Boom, Proceedings of the 9th Symp. on Fus. Techn. (1976), p. 87.
2. R. L. Willig, Sup. MHD Magnet Design Conference (1978).
3. O. Christianson and R. W. Boom, *Adv. in Cryo. Eng.*, **29**, 207 (1970).
4. M. A. Hilal, US-Japan Cooperative Workshop on Superconductive Energy Storage, 19 (1981).
5. H. Desportes et al., *Journal de Physique*, Tome **45 C**,1341 (1984).
6. A. Devred and C. Meuris, Proceedings of the 9th Int. Conf. on Magnet Technology (1985), p. 577.
7. G. Doetsch, "Guide to the Applications of the Laplace and Z-Transforms," Van Nostrand Rheingold Company (London).
8. H. Cartan, "Théories élémentaires des fonctions analytiques d'une ou plusieurs variables complexes," Hermann (Paris).

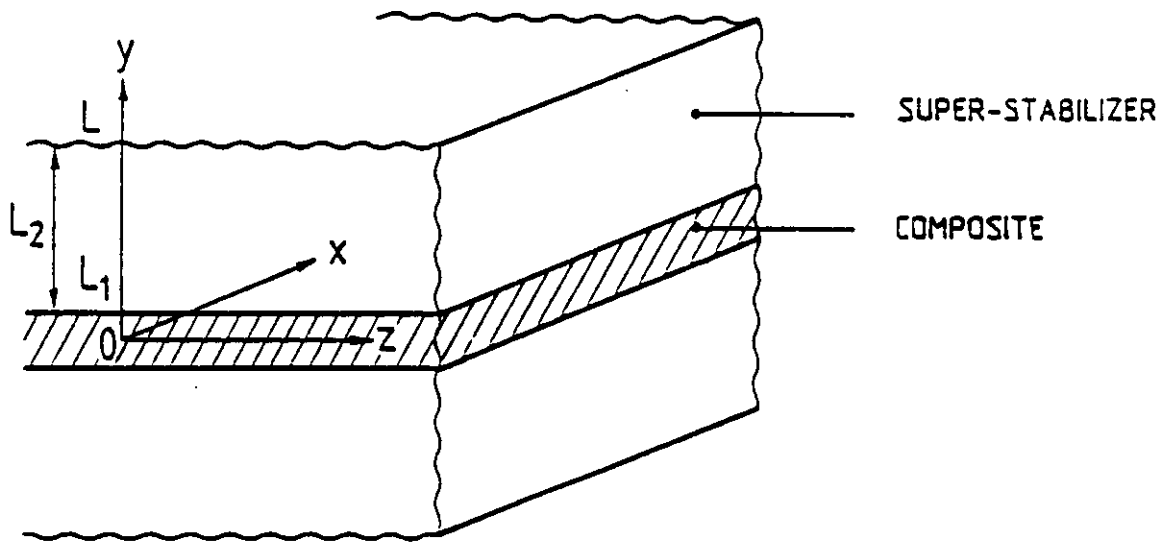
Table I
Numerical Data

$L_1 = 1.1 \text{ mm}$	$\rho_1 = 4.9 \cdot 10^{-10} \text{ } \Omega\text{m}$	$\tau_1 = 0.47 \text{ ms}$
$L_2 = 16.4 \text{ mm}$	$\rho_2 = 7.148 \cdot 10^{-11} \text{ } \Omega\text{m}$	$\tau_2 = 4.6 \text{ s}$
$B_o = -0.87 \text{ T}$	$J_o = 39.7 \text{ A/mm}^2$	$P_{J_o} = 11.8 \cdot 10^6 \text{ W/m}^3$



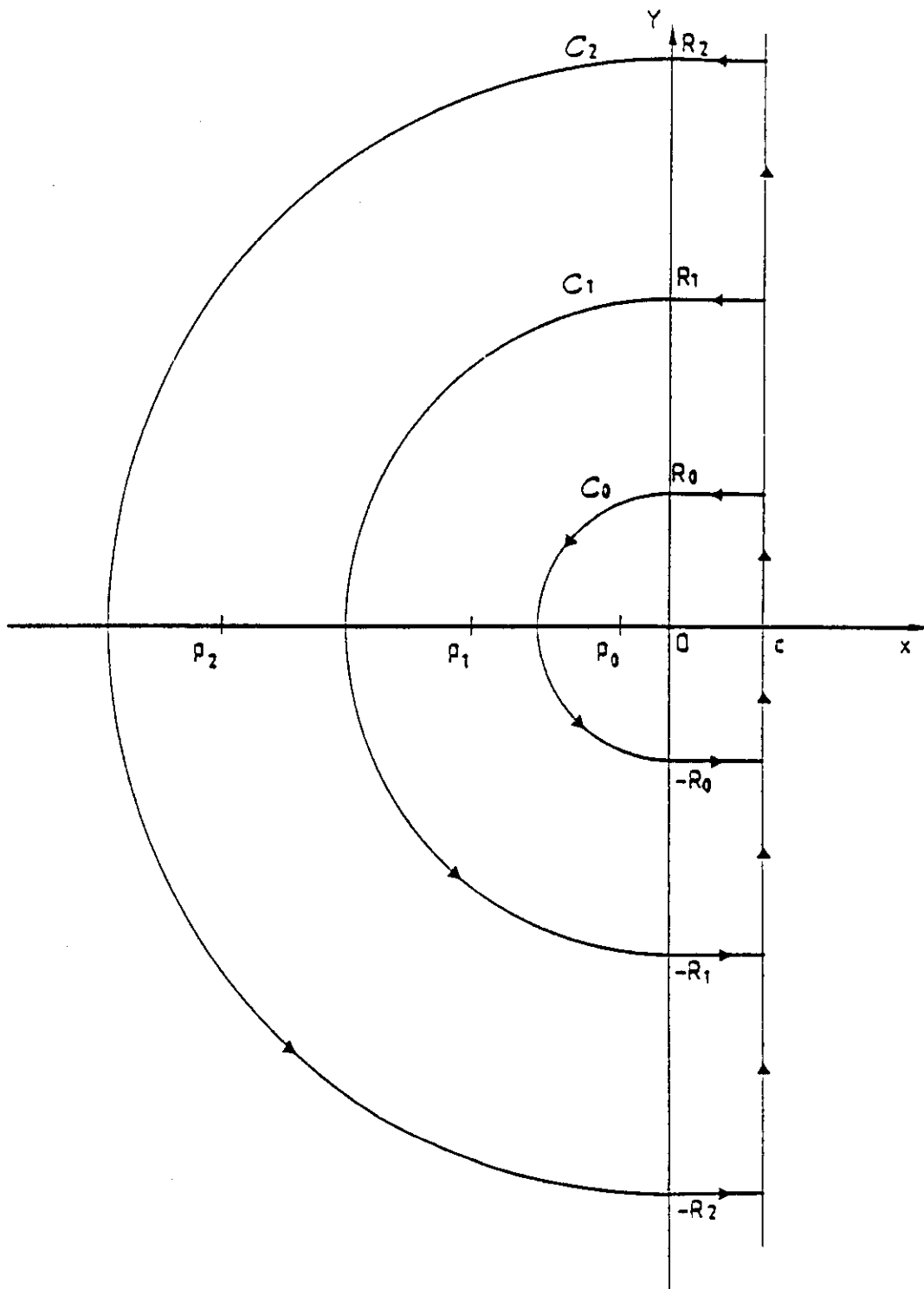
XBL 889-3285

Fig. 1. Sketch of a layer of ALEPH conductors.



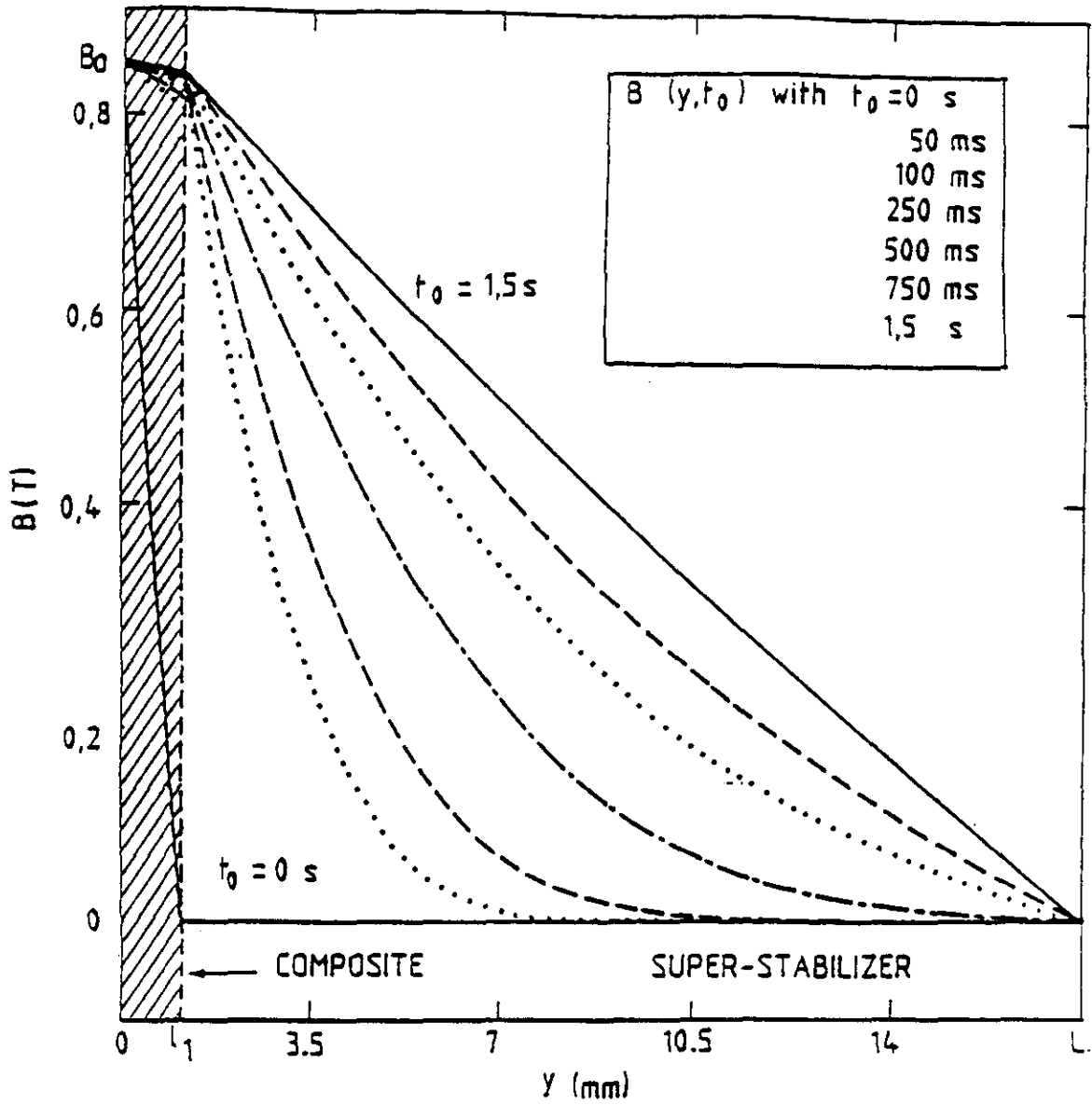
XBL 889-3286

Fig. 2. Infinite plates model.



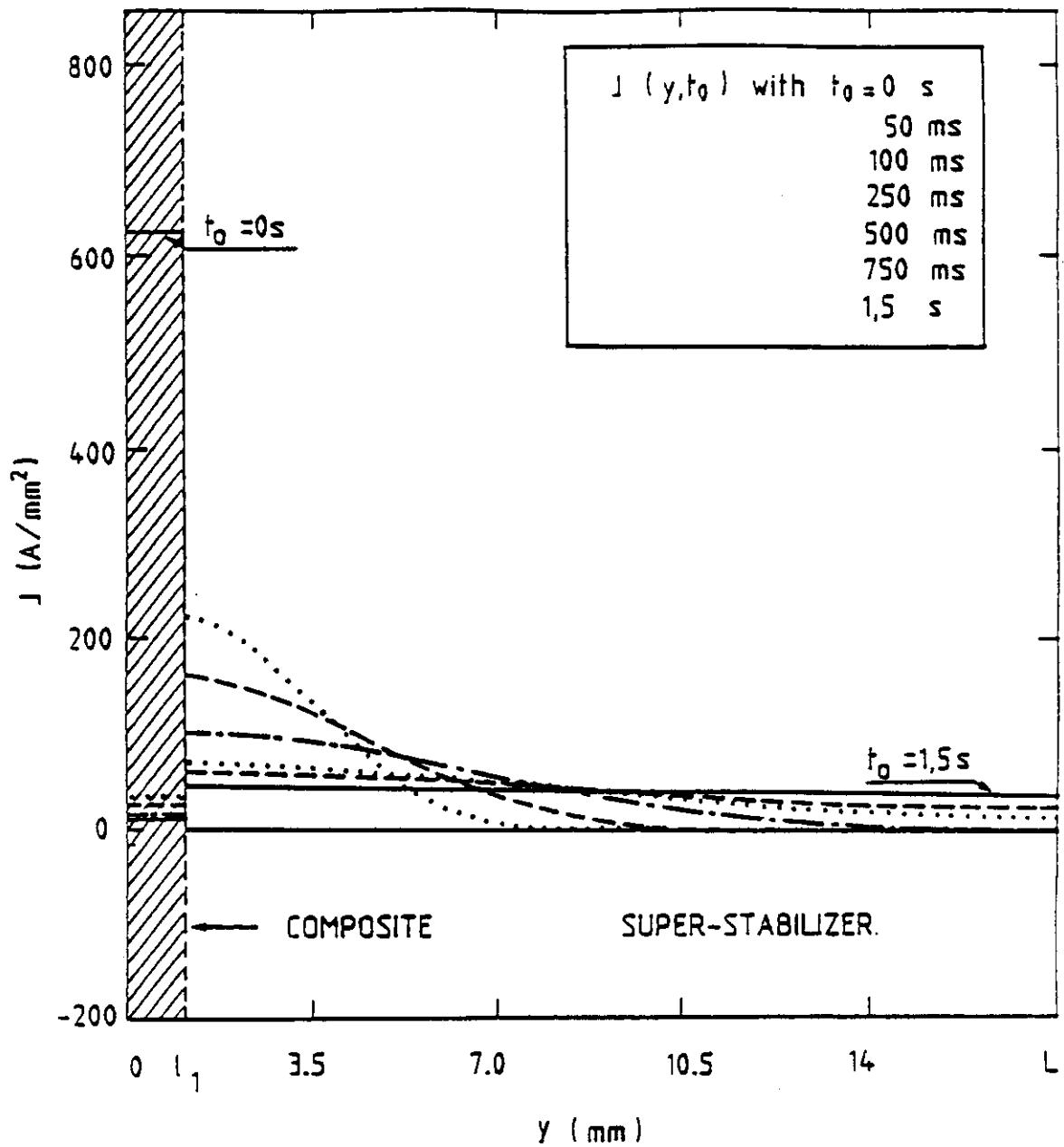
XBL 889-3287

Fig. 3. Contours for the computation of $B_i(y, t)$.



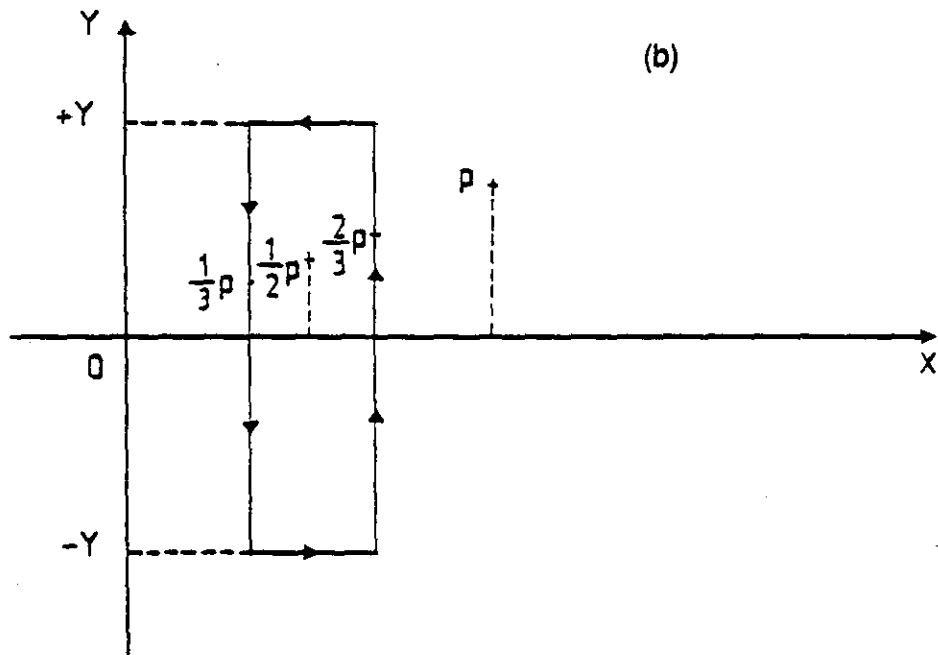
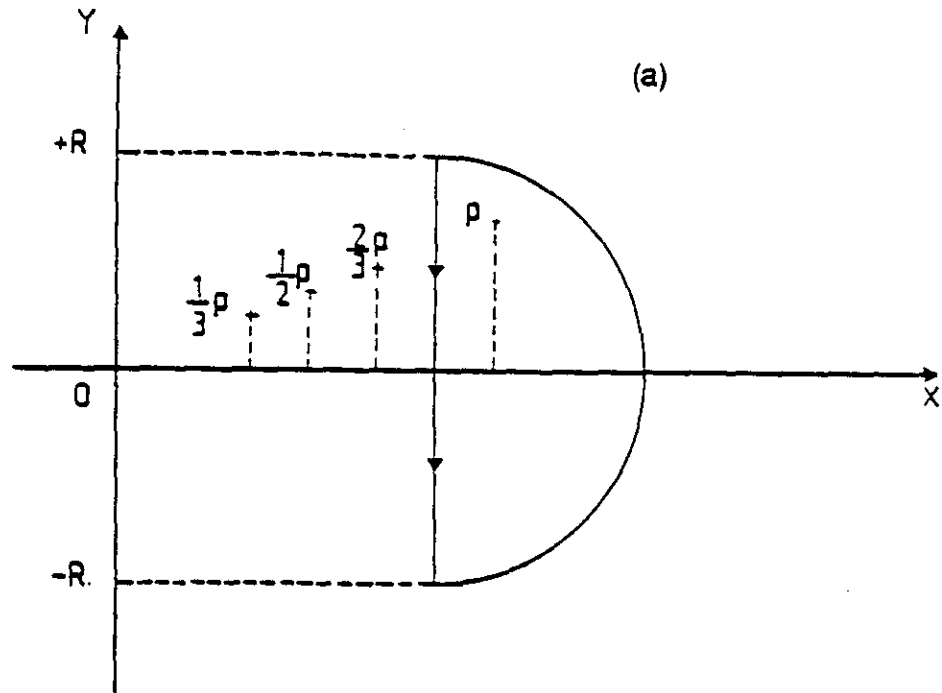
XBL 889-3288

Fig. 4. Profile of magnetic flux density.



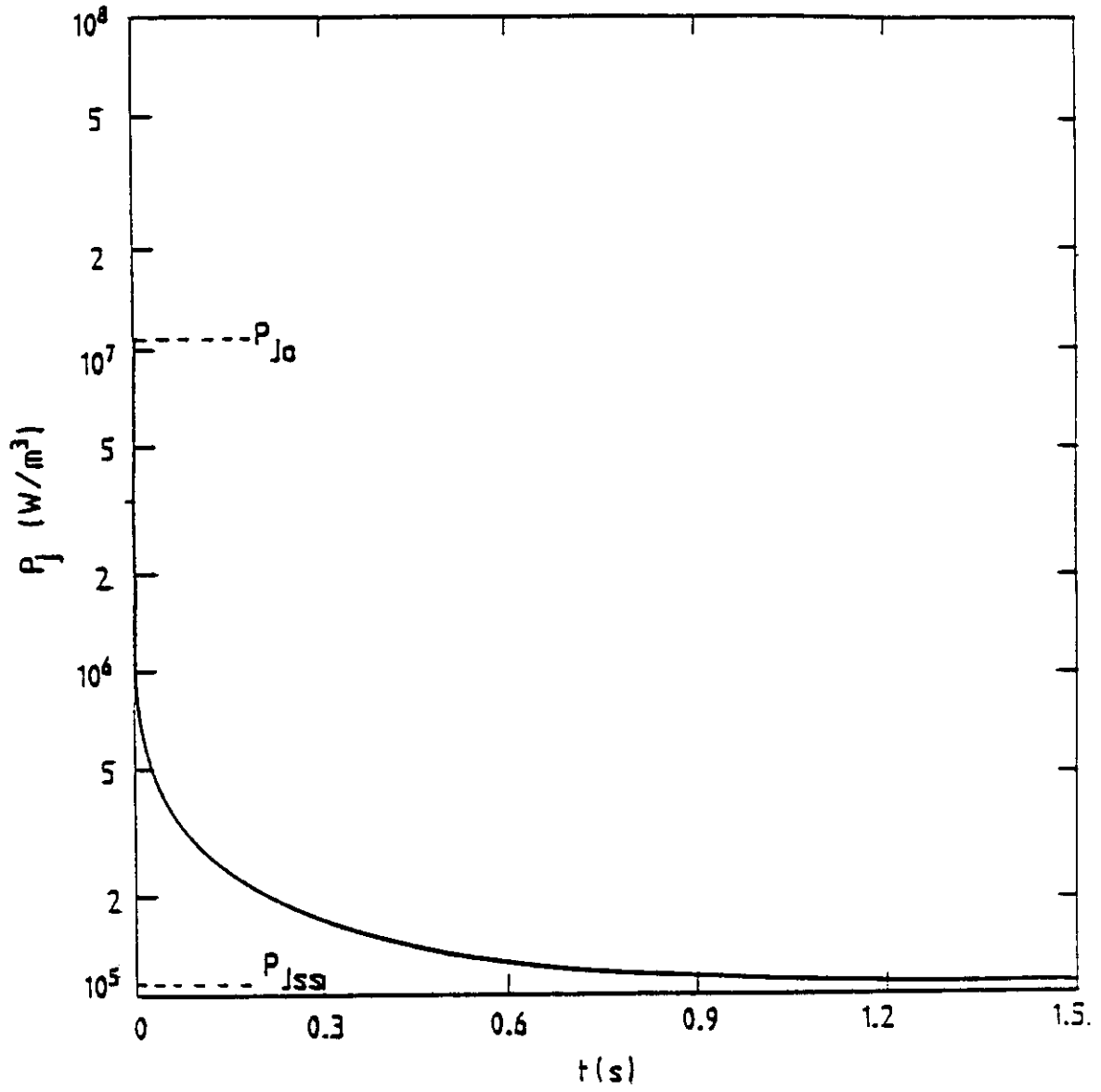
XBL 889-3289

Fig. 5. Profile of current density.



XBL 889-3290

Fig. 6. (a) and (b): Contours for the computation of $I(p)$ and $K(p)$.



XBL 889-3291

Fig. 7. Profile of average generated heat power density.